

Research article

Title

TRAIL Delivered by Mesenchymal Stromal/Stem Cells Counteracts Tumor Development in Orthotopic Ewing Sarcoma Models

Authors

^{1,2} Romain GUIHO, ^{1,2} Kevin BITEAU, ³ Giulia GRISENDI, ^{1,2} Julien TAURELLE, ^{1,2} Mathias CHATELAIS, ^{1,2} Malika GANTIER, ^{1,2} Dominique HEYMANN, ³ Massimo DOMINICI, ^{1,2} Françoise REDINI

Affiliation

¹ INSERM, UMR-957, Equipe labellisée LIGUE contre le CANCER 2012, Nantes, F-44035, France.

² Université de Nantes, EA 3822, Faculté de Médecine, Laboratoire de Physiopathologie de la Résorption Osseuse et thérapie des tumeurs osseuses primitives, Nantes, F-44035, France.

³ Laboratory of Cellular Therapy, Department of Medical and Surgical Sciences for Children & Adults, University Hospital of Modena and Reggio Emilia, Modena, Italy

Contact Information

D^r Françoise REDINI, INSERM UMR957, Faculté de médecine, 1 rue Gaston Veil, 44035 Nantes cedex 1, France

Tel: +33 2 40 41 29 60; fax: +33 2 40 41 28 60

E-mail: francoise.redini@univ-nantes.fr

Novelty & Impact Statements

The benefit of the pro-apoptotic cytokine TNF-Related Apoptosis Inducing Ligand (TRAIL) vectorized by mesenchymal stem cells (MSC) has been reported in a variety of sarcomas. Using several different cell lines *in vitro* and two different orthotropic xenogeneic models we here originally outline how a TRAIL delivery by MSC retains a particular impact against Ewing sarcoma prompting further investigations to assess the safety of a MSC delivery and the raise of possible mechanisms of resistance.

Keywords

TRAIL; Ewing sarcoma; resistance; microenvironment; MSC

This article has been accepted for publication and undergone full peer review but has not been through the copyediting, typesetting, pagination and proofreading process which may lead to differences between this version and the Version of Record. Please cite this article as an 'Accepted Article', doi: 10.1002/ijc.30402

This article is protected by copyright. All rights reserved.

Abstract

Ewing sarcoma (EWS) is the second most frequent pediatric malignant bone tumor. EWS patients have not seen any major therapeutic progress in the last thirty years, in particular in the case of metastatic disease, which requires new therapeutic strategies. The pro-apoptotic cytokine TNF-Related Apoptosis Inducing Ligand (TRAIL) can selectively kill tumor cells while sparing normal cells, making it a promising therapeutic tool in several types of cancer. However, certain EWS cell lines appear resistant to recombinant human (rh) TRAIL-induced apoptosis. We therefore hypothesized that a TRAIL presentation at the surface of the carrier cells might overcome this resistance and trigger apoptosis. For this purpose, human adipose mesenchymal stromal/stem cells (MSC) transfected in a stable manner to express full-length human TRAIL were co-cultured with several human EWS cell lines, inducing apoptosis by cell-to-cell contact even in cell lines initially resistant to rhTRAIL or AMG655, an antibody agonist to the death receptor, DR5. *In vivo*, TRAIL delivered by MSCs was able to counteract tumor progression in two orthotopic models of Ewing sarcoma, associated with caspase activation, indicating that a cell-based delivery of a potent apoptosis-inducing factor could be relevant in EWS.

Introduction

Ewing sarcoma (EWS), the second most common malignant bone tumor in pediatric patients after osteosarcoma, is a rare form of cancer. It is highly metastatic and causes serious disruption to bone remodeling. EWS is identified by a chromosomal translocation between the EWS gene on chromosome 22 and a member of the ETS transcription factor family, more often FLI1 on chromosome 11, leading to production of a fusion protein which behaves like an aberrant transcription factor¹. The resulting fusion protein, EWS-FLI1, directly or indirectly modulates the expression of many genes, altering several cell functions such as cell cycle (by targeting p21/CDKN1A, Cyclin D and E, p57/KIP2, TGF α -, IGF- or MAPK signaling pathways) or apoptosis (by targeting caspase3 and members of the TNF α , IGF-1 and TGF β signaling pathways)². Transformed EWS cells appear as small, round and undifferentiated, and they are involved in major disruption of bone structure, with severe osteolytic lesions.

The current therapeutic approach consists of surgery, neoadjuvant and adjuvant chemotherapy, and in some cases radiotherapy. The 5-year survival rate has barely changed in the past 30 years, and remains at around 70% for localized forms³. However, the rate falls drastically to around 20% for groups of metastatic patients or poor responders to chemotherapy. New avenues of research have been opened by using TNF-Related Apoptosis Inducing Ligand (TRAIL), a pro-apoptotic cytokine from the TNF superfamily. TRAIL can bind to five receptors: two death receptors - TRAIL-R1 (Death Receptor 4: DR4) and TRAIL-R2 (DR5) - two decoy receptors that do not transmit the death signal but that can confer resistance toward TRAIL-induced apoptosis - TRAIL-R3 (Decoy Receptor 1: DcR1) and TRAIL-R4 (DcR2) - and the soluble osteoprotegerin (OPG). TRAIL, by binding to DR4 and DR5, is able to induce apoptosis of tumor cells by activating the recruitment and cleavage of pro-caspase-8 in a complex called Death-Inducing Signaling Complex (DISC). A recruitment and activation cascade leads to tumor cell death by the extrinsic apoptosis pathway. This mechanism can be amplified in certain

cell types by activating the intrinsic apoptosis pathway, depending on the mitochondria and apoptosome. Both pathways lead to the final cleavage of pro-caspase-3 into active caspase-3⁴.

In the early 2000s, it was reported that several cell lines derived from EWS are sensitive to TRAIL-induced apoptosis *in vitro*⁵⁻⁷. Based on these studies, xenograft models showed that recombinant human (rh) TRAIL or death receptor (DR)5 agonists can significantly reduce tumor volume, preventing osteolytic lesions and increasing animal survival^{8,9}. Early clinical trials revealed that rhTRAIL had promising effects, but its sub-optimal bioavailability due to rapid clearance prevented the introduction of rhTRAIL into clinical use^{10,11}. Of the various strategies for increasing the therapeutic effect of TRAIL, using cells carrying TRAIL looks promising¹²⁻¹⁷. These transporter cells can be adipose-derived mesenchymal stromal/stem cells (AD-MSC), modified to encode human TRAIL^{18,19}. Here, we further challenge the promising therapeutic potential of AD-MSC as TRAIL cellular vectors in a variety of EWS cell lines *in vitro*, additionally assessing this anti-cancer gene delivery approach in two different orthotopic *in vivo* models of EWS.

Materials and Methods

Cell cultures

Tumor Cell Lines. Six human EWS cell lines: A-673, SK-N-MC, SK-ES-1, and RD-ES cell lines (kindly provided by Dr S. Burchill, Children's Hospital, Leeds, UK) and EW-24 and TC-71 cell lines (provided by Dr O. Delattre, INSERM U830, Paris, France) were used. The A-673, SK-ES-1, and RD-ES cell lines were cultured in Dulbecco's Modified Eagle's Medium (DMEM, Lonza, Basel, Switzerland) with 5% fetal bovine serum (FBS; Thermo Scientific, Waltham, USA) and 2 mmol/L L-glutamine (Lonza). EW-24, SK-N-MC and TC-71 cells were cultured in Rosewell Park Millenium Institute (RPMI, Lonza) medium with 5% FBS and 2 mmol/L L-glutamine.

Mesenchymal Stromal/Stem Cells. Adipose-Derived (AD)-MSC expressing green fluorescent protein (GFP) only or TRAIL with GFP (named respectively MSC-GFP and MSC-TRAIL) were obtained as previously described^{18,20}. In this setting, AD-MSC were cultured in α MEM (Lonza) supplemented with 10% FBS (Thermo Scientific), 2 mmol/L L-glutamine and 2ng/mL basic Fibroblast Growth Factor (bFGF; R&D Systems, Minneapolis, USA).

In Vitro Experiments

Human TRAIL ELISA Assay. Ninety-six-well plates were coated with polyclonal anti-human TRAIL antibody (0.2 μ g/well, R&D Systems) overnight at room temperature, washed and then incubated for 1 h with a blocking solution (1% bovine serum albumin/Phosphate buffered saline (PBS)). After washing, the wells were incubated at room temperature with supernatant or protein lysate from MSC-GFP and MSC-TRAIL for 2 h, followed by a 2-h incubation with Biotin-SP-conjugated Donkey Anti-Human TRAIL IgG (1:180; R&D Systems). Detection was carried out by incubating the wells with streptavidin-horseradish peroxidase (1:200; R&D systems) for 30 min. The reaction was stopped by adding 50 μ L of 1 mol/L H₂SO₄. Absorbance was then measured at 410nm using a VICTOR2 Multilabel counter (Perkin-Elmer). The ELISA detection limit was 0.02 ng/mL.

Quantitative RT-PCR. Total RNA was extracted from cultured cells (after 48h of treatment) using a Direct-zol™ RNA MiniPrep Kit (Zymo Research). Two µg of total RNA was reverse transcribed using the Maxima H Minus First Strand cDNA Synthesis Kit (Life Technology). Real-time monitoring of complementary DNA (cDNA) PCR amplification was performed using DNA primers on CFX96 (Bio-Rad Laboratories) with SYBRGreen detection according to the manufacturer's recommendations. PCR amplifications involved 39 cycles of 30 s at 98°C, 15s at 95°C and 30s at 60°C. Expression of the target genes was normalized to that of the endogenous control glyceraldehyde 3-phosphate dehydrogenase. The $2\Delta Ct$ (cycle threshold) method was used to calculate expression levels. Gene name symbols with corresponding full names and the list of corresponding primer sequences are indicated in Supplementary Table I.

Cell Growth and Viability. Two thousand tumor cells per well were seeded into 96-well plates and cultured for 72 h in the presence of increasing concentrations (0-1000 ng) of recombinant human TRAIL (rhTRAIL - R&D Systems). Cell growth and viability were determined using a stable tetrazolium salt WST-1 cell proliferation reagent assay kit (Roche, Penzberg, Germany). After the culture period and addition of the WST-1 reagent, the absorbance was then determined at 490 nm. The IC50 were calculated using Graph Pad Prism v6.01 software.

Flow Cytometry Analysis. TRAIL staining: Cells were stained with PE-anti-TRAIL (Biolegend) and isotype controls (Becton Dickinson). Intracellular staining on transduced AD-MSC was performed with a BD Cytofix/Cytoperm kit (Becton Dickinson) using the PE-anti-TRAIL antibody. Annexin V assay: Ten thousand MSC-TRAIL or MSC-GFP cells were seeded into 6-well plates. The next day, tumor cells were added and co-cultured at a tumor cell/AD-MSC ratio of 3:1. After 48h, the cells were detached and stained for the Annexin V assay (BD Bioscience, Franklin Lakes, USA). The percentage of tumor cell apoptosis was quantified by cytometry gating on GFP negative cells with the FC500 flow cytometer (Beckman Coulter, Fullerton, USA).

Effect of MSC supernatant on tumor cells. Five thousand MSC-TRAIL or MSC-GFP cells were seeded into 24-well plates. The next day, two thousand tumor cells were added to Boyden chamber inserts of 3 micron porosity in 24-well plates (BD Bioscience). After 48h, the cells in the inserts were fixed with 2% Glutaraldehyde (Sigma-Aldrich, Saint-Louis, USA) and stained with 0.5% Crystal Violet in ethanol (Sigma-Aldrich). To calculate tumor cell proliferation, the inserts were photographed and the cell surface were analyzed with imageJ software (NIH). The results are reported as a percentage of tumor cell proliferation in the presence of MSC-GFP control.

Caspase 3/7 enzymatic activity

Caspase 3/7 activity was measured using an Apo-ONE® Homogeneous assay kit (Promega). Briefly, cells were lysed in RIPA buffer (10 mM Tris pH8, 1 mM EDTA, 150 mM NaCl, 1% NP40, 0.1% SDS) containing a cocktail of protease and phosphatase inhibitors (1 mM sodium orthovanadate (Na₂VO₄), 1 mM phenylmethylsulfonyl fluoride (PMSF), 10 mM sodium fluoride (NaF), 10 mM N-ethylmaleimide (NEM), 2 µg/ml leupeptin and 1 µg/ml pepstatine) at 4°C. An equal volume of reagents was added to a white-walled 96-well plate containing protein extracts and incubated at room temperature for 16h. The fluorescence of each sample was measured in a plate-reading Tristar LB941 (Berthold technologies). The data shown concern the concentration of total protein determined with a BCA kit (Sigma, St Quentin-Fallavier, France).

***In Vivo* Experiments**

Ewing sarcoma animal models. Four-week-old Rj:NMRI-nude mice (Janvier Labs - Le Genest-Saint-Isle, France) were housed under pathogen-free conditions at the Experimental Therapy Unit (Faculty of Medicine, Nantes, France) in accordance with the institutional guidelines of the French Ethical Committee (CEEA Pays de la Loire n°6) and under the supervision of authorized investigators (protocol authorization n°1281.01). The mice were anesthetized by inhalation of an isoflurane/air mixture before receiving an intramuscular injection of 10⁶ TC-71 or A-673 EWS cells in close proximity

to the tibia. The tumor volume (V) was calculated by measuring three perpendicular diameters with a caliper, according to the following formula: $V = 0.5 \times \text{length} \times \text{width} \times \text{height}$. The mice were sacrificed for ethical reasons when tumor volume reached 1 800 mm³.

Histology. One million MSC-TRAIL or MSC-GFP were injected into established tumors of approximately 200 mm³. After 24h, tumor specimens were fixed in formalin and embedded in paraffin by conventional techniques. Immunofluorescence double staining with a sequential approach was used to demonstrate the simultaneous presence of cleaved-caspase-3 (CC3) and GFP (modified MSC) in the tumor. Tissue sections (3µm) were blocked (Blocking reagent 1) and pretreated in pH6 citrate buffer. Slides were incubated at 20°C with CC3 primary antibody then with A957-conjugated secondary antibody. Slides were blocked at 4°C overnight with IgG Fab goat anti-rabbit. Sections were incubated at 20°C with GFP primary antibody then with A488-conjugated secondary antibody. Slides were mounted in Prolong Gold antifading reagent with DAPI (Molecular Probes – P36935). The primary antibodies, fluorochrome-conjugated antibodies and blocking reagent used in this study are listed in Supplementary Table II. Fluorescence was visualized using an Axiovert 200 M microscopy system (Zeiss, Le Pecq, France) with the ApoTome module (x63) or with a fluorescent slide scanner (Nanozoomer, Hamamatsu).

Statistical analyses

Each experiment was repeated independently 3 times. The results are given as a mean ± SD for *in vitro* experiments and a mean ± SEM for *in vivo* experiments. They were compared using an unpaired t test or two-way ANOVA followed respectively by the Bonferroni post-test or the Tukey's multiple comparisons test using Graph Pad Prism v6.01 software. Results with $p < 0.05$ were considered significant and are represented by an asterisk (*), $p < 0.01$ results are represented by two asterisks (**) and $p < 0.001$ by three asterisks (***)

Results

Confirmation of GFP and TRAIL transduction efficiency in MSC-GFP and MSC-TRAIL. AD-MSC were transduced in a stable manner with vector encoding full-length human TRAIL (MIGR1-TRAIL-GFP) and with control vector (MIGR1-GFP). After 3 passages, fluorescent microscopy (**Figure 1A**) and cytometry analysis (**Figure 1B**) confirmed that more than 98% of the transduced MSC were GFP positive. RT-qPCR analyses showed that MSC-GFP constitutively expressed negligible TRAIL mRNA levels (**Figure 1C**), with protein levels that were below the ELISA detection limit (**Figure 1D**). In contrast, gene modification of the MSCs with TRAIL-encoding vector made high mRNA levels possible (**Figure 1C**), as well as relevant protein expression (8 ng/mg protein extract, **Figure 1D**). However, very small amounts of soluble TRAIL, around 0.1 ng/mL after 48h, were recovered from the supernatant (**Figure 1E**), indirectly indicating that TRAIL is mainly expressed in its membrane form. This was confirmed by flow cytometry analysis, showing that TRAIL expression was exclusively present in AD-MSC TRAIL, both as a surface and an intracellular protein (**Figure 1F**).

AD-MSC delivering TRAIL was able to overcome rhTRAIL resistance in six Ewing sarcoma cell lines. Proliferation assays in the presence of rhTRAIL showed that the EWS cell lines studied did not respond to rhTRAIL to the same extent (**Figure 2A**): Ewing sarcoma cell lines TC-71 and RD-ES were highly sensitive to the anti-proliferative effect of rhTRAIL ($IC_{50} < 200\text{ng/mL}$), A-673 and SK-N-MC cell lines were less responsive with an $IC_{50} < 1000\text{ng/mL}$. This pro-apoptotic effect was confirmed by caspase-3 enzymatic activity (**Figure 2B**). The other cell lines (EW-24 and SK-ES-1) were resistant to the highest rhTRAIL concentration ($IC_{50} > 1000\text{ng/mL}$).

On the contrary, when the EWS cell lines were challenged by TRAIL delivered by AD-MSC (**Figure 3 A, B**), all cell lines showed induction of apoptosis, even the initially rhTRAIL-resistant cell lines. This sensitivity was demonstrated by apoptosis cytometry assay for two representative cases: rhTRAIL-sensitive TC-71 and rhTRAIL-resistant SK-ES-1 cells (**Figure 3A**).

We then decided to assess whether this anti-cancer effect was mediated by membrane- or soluble forms of TRAIL, or both (**Figure 3C**). Tumor cells in Boyden chambers overhanging MSC-TRAIL did not slow their proliferation when compared to tumor cells in Boyden chambers overhanging MSC-GFP (illustration for TC-71 and SK-ES-1 in **Figure 3D**). These results show that a direct cell-to-cell contact between EWS cells and MSC-TRAIL is necessary for cell death to be induced, indirectly suggesting that the amount of TRAIL released by MSC-TRAIL is not enough to reduce proliferation in cell lines.

MSC-TRAIL inhibit tumor progression when co-injected with EWS cells *in vivo* in two orthotopic models. Based on *in vitro* data showing that TC-71 cells have the highest sensitivity to both rhTRAIL and MSC-TRAIL, we developed a para-tibial orthotopic tumor model to verify the impact of MSC-TRAIL *in vivo* in the relevant corresponding animal model. Either 10^6 TC-71 cells alone or TC-71 combined with 10^6 of MSC-TRAIL or MSC-GFP were injected once at Day 0 (D0). The group inoculated with MSC-GFP showed the same tumor progression as the control group (**Figure 4A**). On the contrary, one dose of MSC-TRAIL injection was enough to abolish tumor development by 75% on tumor growth starting from D20 (**Figure 4A, B**). This was associated with a significant impact on survival rate (calculated when tumor volume reached 1500 mm^3), which increased by 60% in the group co-injected with MSC-TRAIL (**Figure 4C**). Macroscopic pulmonary metastases were not detected in any of the groups studied (**Figure 4D**). After 26 days of tumor proliferation, tumor cell isolation in the MSC-GFP treated group showed that less than 0.25% of the cells were GFP positive, indicating that MSC did not proliferate in tumors (**Figure 4E**).

To further challenge the MSC-TRAIL strategy, we established an additional para-tibial orthotopic tumor model using the highly proliferating A-673 line that showed less sensitivity to rhTRAIL than TC-71 cells. Thus, 10^6 A-673 cells alone or with one dose of 10^6 of MSC-TRAIL or MSC-GFP were injected at D0. The A-673 line confirmed its aggressiveness *in vivo*, with rapid generation of large tumors in less than 20 days (**Figure 5A, B**). Although there was no difference in the survival rate of the mice (calculated when tumor volume reached 1200 mm^3) injected with A-673 alone or A-673 with MSC-

GFP (**Figure 4C**), the group co-injected with MSC-GFP showed a slight, though significant, acceleration in tumor growth when compared to the control group (**Figure 5A, B**). Despite the pro-tumoral effect of MSC-GFP, the injection with MSC-TRAIL controlled tumor growth and tumors were barely detectable in the MSC-TRAIL group, with a tumor volume of less than 80 mm³ at 20 days (**Figure 5A, B**). As a consequence, the survival rate increased significantly in the group co-injected with MSC-TRAIL and A-673 cells, and the mice developed significant tumor volumes only 40 days after the injection time, surviving for more than 70 days, despite the aggressiveness of the A-673 cell line (**Figure 5C**).

However, when MSC-TRAIL were injected into established tumors, only a transient significant inhibitory effect could be observed around day 5, but this did not affect animal survival (**Supplementary Figure S1**).

***In vivo* MSC-TRAIL induce apoptosis in adjacent Ewing sarcoma tumor cells.** To investigate the anti-tumorigenic effect of MSC-TRAIL *in situ*, mice were injected with A-673 cells to generate tumors rapidly. When their volume reached 200 mm³, either one million MSC-GFP or MSC-TRAIL were injected into the tumors (n=3). Immunofluorescence analyses of the EWS model showed that MSC-TRAIL injected into the tumor were able to induce apoptosis of adjacent A-673 EWS cells, as revealed by the detection of cleaved caspase-3 by immunofluorescence (**Figure 5D**). This effect remained local, as the presence of active caspase-3 was only localized around the injected MSC-TRAIL on a total histological section of the tumor (**Figure 5E**). On the contrary, MSC-GFP injection did not induce apoptosis in adjacent EWS cells.

Discussion

The ability of TRAIL to induce tumor apoptosis and death without affecting normal cells makes it a very interesting tool for tumor therapy. However, many types of cancer remain resistant to TRAIL, including sarcomas^{21,22}. Finding relevant and diversified strategies to overcome this resistance seems to be an essential prerequisite for offering patients new therapeutic options.

MSC can be engineered to express TRAIL and a recent study has demonstrated that these cells can induce apoptosis in a variety of sarcomas (osteosarcoma, rhabdomyosarcoma, EWS) by activation of caspase-8²⁰, paving the way for MSC-TRAIL-based therapies in these still deadly forms of cancer. Here, we further confirm these findings by focusing on EWS and demonstrating that AD-MSC delivering TRAIL can induce apoptosis in a wide panel of EWS cell lines *in vitro*. All the cell lines considered were sensitive to apoptosis induced by MSC-TRAIL, suggesting that the extrinsic apoptosis signaling pathway is functional in all these cell lines. This appears to be in contrast with the data, suggesting that some of these lines are resistant to relatively high amounts of rhTRAIL. While this finding requires further investigation, we can currently hypothesize that MSC-TRAIL is able to induce significant clustering of death receptors at the surface of EWS cells, multiplying the downstream activation of caspase-8. A study with liposome-bound TRAIL reports that higher DR5 clustering enhances DISC formation and triggers caspase activation more efficiently than the soluble form of rhTRAIL²³. In addition, a second TRAIL signaling pathway has recently been described, involving NF- κ B, MAPK, PI3K/Akt activation via binding to the same receptors, but leading to increased tumor cell proliferation, survival, migration and invasion (reviewed in²⁴). The key regulator of this kinase network is the RIPK1 protein, which binds FADD instead of caspase-8, inducing the formation of a secondary signaling complex composed of TRADD, TRAF2 and RIPK1. We can further hypothesize that rhTRAIL can activate this secondary pathway that counteracts its pro-apoptotic effect, whereas high clustering of MSC-TRAIL and death receptors may associate several caspase-8 molecules which overcome the formation of the RIPK1-TRADD-TRAF2 complex. The evidence that only direct contact

between EWS cells and MSC-TRAIL can induce apoptosis supports the concept that a high level of death receptor clustering is necessary for apoptosis induction *via* DISC formation. The need for cell-to-cell contact for AD-MSC TRAIL delivery has been also reported in a cervical carcinoma cell line¹⁸. However, our study is the first evidence provided in several sarcoma cell lines, indicating that a cell delivery approach for TRAIL may be far more efficient than rhTRAIL alone, indicating the need for dedicated strategies to drive MSC homing and persistence inside tumors.

A previous study showed that MSC-TRAIL can exert relevant antitumor activity against a subcutaneous xenograft model of RD-ES EWS cells²⁰. However, we felt that in these neoplastic disorders so closely related to skeletal tissues, more relevant orthotopic models needed to be introduced, taking into account their peculiar tumor microenvironment. For this reason, we introduced two different para-tibial orthotopic EWS models. Confirming early data obtained in a EWS sub-cutaneous model, tumor progression was counteracted by a single dose of MSC-TRAIL, underlining the therapeutic potential of this approach and indicating the need for delivery optimization with a different schedule (multiple deliveries) for MSC-TRAIL or with MSC delivering soluble variants of TRAIL.

It has been shown that MSC expressing TRAIL were able to reduce the incidence of lung metastases in carcinoma models¹⁵. However, this effect was not observed in our EWS mouse models as the cells were highly aggressive with too rapid progression that was not enough to develop and observe spontaneous metastases. We therefore cannot conclude on the effect of MSC-TRAIL on the occurrence of metastases in these models, and dedicated EWS metastatic models are needed to clarify this aspect.

We also report that in one of the para-tibial orthotopic EWS model obtained with the A-673 EWS line, the MSC-GFP enhanced tumor progression, as previously described with the HeLa cell line¹⁸. Several studies have reported that MSC may have the ability to promote cancer growth, particularly by increasing angiogenesis, releasing chemokines or interfering with cancer metabolism²⁵⁻²⁸. This

Accepted Article

effect observed in osteosarcoma syngeneic and xenograft mouse models^{29,30} seems to be an obstacle to the use of MSCs as therapeutic tools in bone tumor pathologies. However, other results suggest that MSCs inhibit tumor growth, especially by inhibiting the Wnt pathway³¹⁻³⁵. A concise review categorizes both MSC pro- or anti-tumor effects depending on different tumor types and microenvironments³⁶. Therefore, understanding the conditions in which MSC may enhance tumor growth is crucial for safely developing MSCs as a therapeutic tool.

In conclusion, we have shown that AD-MSCs delivering TRAIL can counteract EWS growth both *in vitro* and *in vivo* within two different orthotopic EWS models. Efforts will now focus on solidifying the strategy in order to safely transfer MSCs as therapeutic tools for EWS, starting with deeper understanding of the conditions in which MSCs may influence tumor growth before properly defining delivery approaches. However, the use of MSC-TRAIL evidenced that a high death receptor membrane presentation is able to induce apoptosis in cell lines initially resistant to rhTRAIL *in vitro*. This clustering strategy is very promising and can be conducted with more neutral TRAIL vectors, such as new TRAIL death receptor agonists capable of bind six receptors³⁷.

Acknowledgements

This study received funding from LA LIGUE CONTRE LE CANCER. In addition, this project was carried out thanks to the support of the FÉDÉRATION ENFANTS ET SANTÉ and the SOCIÉTÉ FRANÇAISE DE LUTTE CONTRE LES CANCERS ET LES LEUCÉMIES DE L'ENFANT ET DE L'ADOLESCENT. This project was conducted with financial support from the association ÉTOILE DE MARTIN (RG).

This work was supported in part by: the Associazione Italiana Ricerca Cancro (AIRC) IG 2012 Grant#12755 (MD); the Ministero Italiano Istruzione Università e Ricerca PRIN 2008WECX78 (MD); the Ministero della Salute Bando GR-2008-1145964 (MD) and the Associazione ASEOP (MD, GG).

Disclosure of Potential Conflicts of Interest

None declared.

Accepted Article

References

1. Pinto A, Dickman P, Parham D. Pathobiologic markers of the ewing sarcoma family of tumors: state of the art and prediction of behaviour. *Sarcoma* 2011;2011:856190.
2. Stoll G, Surdez D, Tirode F, Laud K, Barillot E, Zinovyev A, Delattre O. Systems biology of Ewing sarcoma: a network model of EWS-FLI1 effect on proliferation and apoptosis. *Nucleic Acids Res* 2013;41:8853–71.
3. Womer RB, West DC, Krailo MD, Dickman PS, Pawel BR, Grier HE, Marcus K, Sailer S, Healey JH, Dormans JP, Weiss AR. Randomized Controlled Trial of Interval-Compressed Chemotherapy for the Treatment of Localized Ewing Sarcoma: A Report From the Children's Oncology Group. *Journal of Clinical Oncology* 2012;30:4148–54.
4. Ozören N, El-Deiry WS. Defining characteristics of Types I and II apoptotic cells in response to TRAIL. *Neoplasia* 2002;4:551–7.
5. Kontny HU, Hämmerle K, Klein R, Shayan P, Mackall CL, Niemeyer CM. Sensitivity of Ewing's sarcoma to TRAIL-induced apoptosis. *Cell Death Differ* 2001;8:506–14.
6. Mitsiades N, Poulaki V, Mitsiades C, Tsokos M. Ewing's sarcoma family tumors are sensitive to tumor necrosis factor-related apoptosis-inducing ligand and express death receptor 4 and death receptor 5. *Cancer Res* 2001;61:2704–12.
7. Van Valen F, Fulda S, Truckenbrod B, Eckervogt V, Sonnemann J, Hillmann A, Rödl R, Hoffmann C, Winkelmann W, Schäfer L, Dockhorn-Dworniczak B, Wessel T, Boos J, Debatin KM, Jürgens H. Apoptotic responsiveness of the Ewing's sarcoma family of tumours to tumour necrosis factor-related apoptosis-inducing ligand (TRAIL). *Int J Cancer* 2000;88:252–9.
8. Merchant MS, Yang X, Melchionda F, Romero M, Klein R, Thiele CJ, Tsokos M, Kontny HU, Mackall CL. Interferon gamma enhances the effectiveness of tumor necrosis factor-related apoptosis-inducing ligand receptor agonists in a xenograft model of Ewing's sarcoma. *Cancer Res* 2004;64:8349–56.
9. Picarda G, Lamoureux F, Geffroy L, Delepine P, Montier T, Laud K, Tirode F, Delattre O, Heymann D, Rédini F. Preclinical evidence that use of TRAIL in Ewing's sarcoma and osteosarcoma therapy inhibits tumor growth, prevents osteolysis, and increases animal survival. *Clin Cancer Res* 2010;16:2363–74.
10. Kelley SK, Harris LA, Xie D, Deforge L, Totpal K, Bussiere J, Fox JA. Preclinical studies to predict the disposition of Apo2L/tumor necrosis factor-related apoptosis-inducing ligand in humans: characterization of in vivo efficacy, pharmacokinetics, and safety. *J Pharmacol Exp Ther* 2001;299:31–8.
11. Ashkenazi A, Holland P, Eckhardt SG. Ligand-based targeting of apoptosis in cancer: the potential of recombinant human apoptosis ligand 2/Tumor necrosis factor-related apoptosis-inducing ligand (rhApo2L/TRAIL). *J Clin Oncol* 2008;26:3621–30.
12. Sasportas LS, Kasmieh R, Wakimoto H, Hingtgen S, van de Water JAJM, Mohapatra G, Figueiredo JL, Martuza RL, Weissleder R, Shah K. Assessment of therapeutic efficacy and fate of

- engineered human mesenchymal stem cells for cancer therapy. *Proc Natl Acad Sci USA* 2009;106:4822–7.
13. Barti-Juhász H, Mihalik R, Nagy K, Grisendi G, Dominici M, Petak I. Bone marrow derived mesenchymal stem/stromal cells transduced with full length human TRAIL repress the growth of rhabdomyosarcoma cells in vitro. *Haematologica* 2011;96:e21–2.
 14. Carlo-Stella C, Lavazza C, Nicola MD, Cleris L, Longoni P, Milanese M, Magni M, Morelli D, Gloghini A, Carbone A, Gianni AM. Antitumor Activity of Human CD34+ Cells Expressing Membrane-Bound Tumor Necrosis Factor-Related Apoptosis-Inducing Ligand. *Human Gene Therapy* 2006;17:1225–40.
 15. Loebinger MR, Eddaoudi A, Davies D, Janes SM. Mesenchymal Stem Cell Delivery of TRAIL Can Eliminate Metastatic Cancer. *Cancer Res* 2009;69:4134–42.
 16. Mohr A, Lyons M, Deedigan L, Harte T, Shaw G, Howard L, Barry F, O'Brien T, Zwacka R. Mesenchymal stem cells expressing TRAIL lead to tumour growth inhibition in an experimental lung cancer model. *Journal of Cellular and Molecular Medicine* 2008;12:2628–43.
 17. Yuan Z, Kolluri KK, Sage EK, Gowers KHC, Janes SM. Mesenchymal stromal cell delivery of full-length tumor necrosis factor-related apoptosis-inducing ligand is superior to soluble type for cancer therapy. *Cytotherapy* 2015;
 18. Grisendi G, Bussolari R, Cafarelli L, Petak I, Rasini V, Veronesi E, De Santis G, Spano C, Tagliazucchi M, Barti-Juhász H, Scarabelli L, Bambi F, Frassoldati A, Rossi G, Casali C, Morandi U, Horwitz EM, Paolucci P, Conte P, Dominici M. Adipose-derived mesenchymal stem cells as stable source of tumor necrosis factor-related apoptosis-inducing ligand delivery for cancer therapy. *Cancer Res* 2010;70:3718–29.
 19. Ciavarella S, Grisendi G, Dominici M, Tucci M, Brunetti O, Dammacco F, Silvestris F. In vitro anti-myeloma activity of TRAIL-expressing adipose-derived mesenchymal stem cells. *Br J Haematol* 2012;157:586–98.
 20. Grisendi G, Spano C, D'souza N, Rasini V, Veronesi E, Prapa M, Petrachi T, Piccinno S, Rossignoli F, Burns JS, Fiorcari S, Granchi D, Baldini N, Horwitz EM, Guarneri V, Conte P, Paolucci P, Dominici M. Mesenchymal progenitors expressing TRAIL induce apoptosis in sarcomas. *Stem Cells* 2015;33:859–69.
 21. Picarda G, Trichet V, Téletchéa S, Heymann D, Rédini F. TRAIL receptor signaling and therapeutic option in bone tumors: the trap of the bone microenvironment. *Am J Cancer Res* 2012;2:45–64.
 22. Guiho R, Biteau K, Heymann D, Redini F. TRAIL-based therapy in pediatric bone tumors: how to overcome resistance. *Future Oncol* 2015;11:535–42.
 23. De Miguel D, Gallego-Lleyda A, Anel A, Martinez-Lostao L. Liposome-bound TRAIL induces superior DR5 clustering and enhanced DISC recruitment in histiocytic lymphoma U937 cells. *Leuk Res* 2015;
 24. Azijli K, Weyhenmeyer B, Peters GJ, de Jong S, Kruyt FAE. Non-canonical kinase signaling by the death ligand TRAIL in cancer cells: discord in the death receptor family. *Cell Death Differ* 2013;20:858–68.

25. Karnoub AE, Dash AB, Vo AP, Sullivan A, Brooks MW, Bell GW, Richardson AL, Polyak K, Tubo R, Weinberg RA. Mesenchymal stem cells within tumour stroma promote breast cancer metastasis. *Nature* 2007;449:557–63.
26. Yu JM, Jun ES, Bae YC, Jung JS. Mesenchymal stem cells derived from human adipose tissues favor tumor cell growth in vivo. *Stem Cells Dev* 2008;17:463–73.
27. Zhu W, Xu W, Jiang R, Qian H, Chen M, Hu J, Cao W, Han C, Chen Y. Mesenchymal stem cells derived from bone marrow favor tumor cell growth in vivo. *Exp Mol Pathol* 2006;80:267–74.
28. Bonuccelli G, Avnet S, Grisendi G, Salerno M, Granchi D, Dominici M, Kusuzaki K, Baldini N. Role of mesenchymal stem cells in osteosarcoma and metabolic reprogramming of tumor cells. *Oncotarget* 2014;5:7575–88.
29. Perrot P, Rousseau J, Bouffaut A-L, Rédini F, Cassagnau E, Deschaseaux F, Heymann M-F, Heymann D, Duteille F, Trichet V, Gouin F. Safety concern between autologous fat graft, mesenchymal stem cell and osteosarcoma recurrence. *PLoS ONE* 2010;5:e10999.
30. Avril P, Le Nail L-R, Brennan MÁ, Rosset P, De Pinieux G, Layrolle P, Heymann D, Perrot P, Trichet V. Mesenchymal stem cells increase proliferation but do not change quiescent state of osteosarcoma cells: Potential implications according to the tumor resection status. *Journal of Bone Oncology* 2016;5:5–14.
31. Qiao L, Xu Z-L, Zhao T-J, Ye L-H, Zhang X-D. Dkk-1 secreted by mesenchymal stem cells inhibits growth of breast cancer cells via depression of Wnt signalling. *Cancer Lett* 2008;269:67–77.
32. Qiao L, Xu Z, Zhao T, Zhao Z, Shi M, Zhao RC, Ye L, Zhang X. Suppression of tumorigenesis by human mesenchymal stem cells in a hepatoma model. *Cell Res* 2008;18:500–7.
33. Zhu Y, Sun Z, Han Q, Liao L, Wang J, Bian C, Li J, Yan X, Liu Y, Shao C, Zhao RC. Human mesenchymal stem cells inhibit cancer cell proliferation by secreting DKK-1. *Leukemia* 2009;23:925–33.
34. Secchiero P, Zorzet S, Tripodo C, Corallini F, Melloni E, Caruso L, Bosco R, Ingraio S, Zavan B, Zauli G. Human bone marrow mesenchymal stem cells display anti-cancer activity in SCID mice bearing disseminated non-Hodgkin's lymphoma xenografts. *PLoS ONE* 2010;5:e11140.
35. Khakoo AY, Pati S, Anderson SA, Reid W, Elshal MF, Rovira II, Nguyen AT, Malide D, Combs CA, Hall G, Zhang J, Raffeld M, Rogers TB, Stetler-Stevenson W, Frank JA, Reitz M, Finkel T. Human mesenchymal stem cells exert potent antitumorigenic effects in a model of Kaposi's sarcoma. *J Exp Med* 2006;203:1235–47.
36. Klopp AH, Gupta A, Spaeth E, Andreeff M, Marini F. Concise review: Dissecting a discrepancy in the literature: do mesenchymal stem cells support or suppress tumor growth? *Stem Cells* 2011;29:11–9.
37. Gieffers C, Kluge M, Merz C, Sykora J, Thiemann M, Schaal R, Fischer C, Branschädel M, Abhari BA, Hohenberger P, Fulda S, Fricke H, Hill O. APG350 induces superior clustering of TRAIL receptors and shows therapeutic antitumor efficacy independent of cross-linking via Fcγ receptors. *Mol Cancer Ther* 2013;12:2735–47.

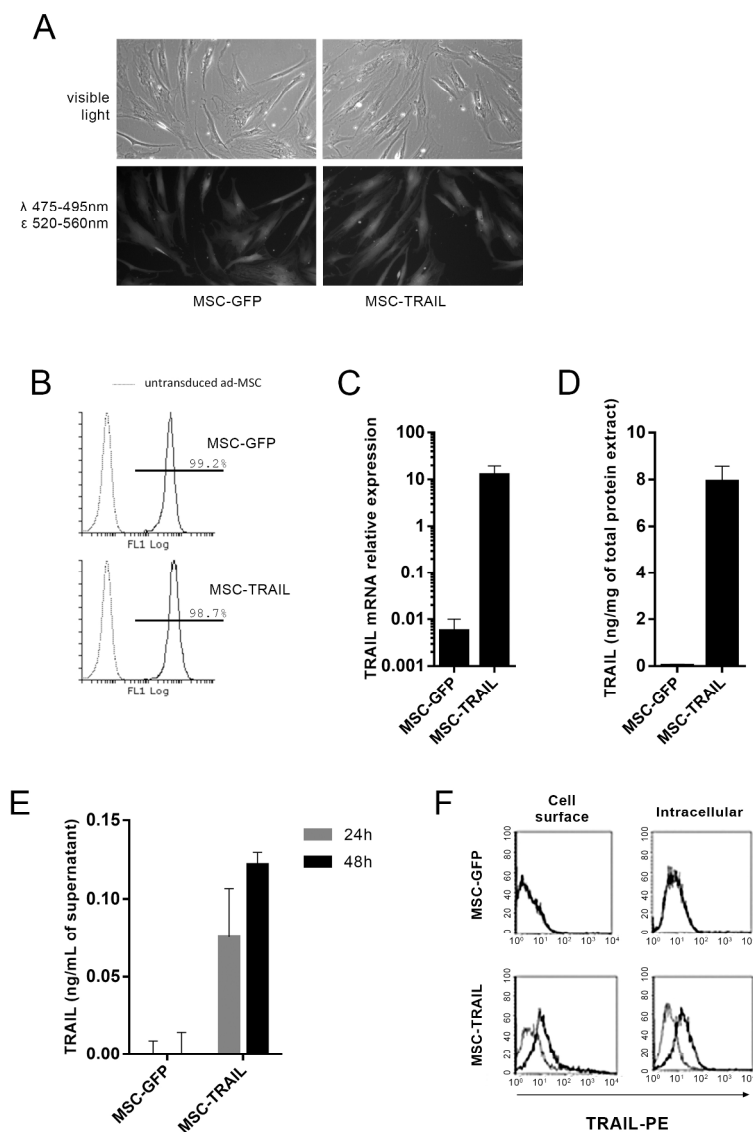


Figure 1. Characterization of transduced MSC.

- A. Confirmation of transduced cells by observation of MSC-GFP and MSC-TRAIL using fluorescence microscopy.
- B. Flow cytometry analysis of MSC-GFP and MSC-TRAIL compared to non-transduced ad-MSC, monitored with the FL1 channel.
- C. RT-qPCR analysis of MSC-GFP and MSC-TRAIL for TRAIL mRNA expression, compared to the reference gene: GAPDH.
- D. TRAIL protein analysis using ELISA of MSC-GFP and MSC-TRAIL total protein extract.
- E. TRAIL analysis using ELISA in MSC-GFP and MSC-TRAIL supernatant after 24 or 48h of culture.
- F. TRAIL membranous and intracellular expression by flow cytometry.

Figure 1

209x297mm (300 x 300 DPI)

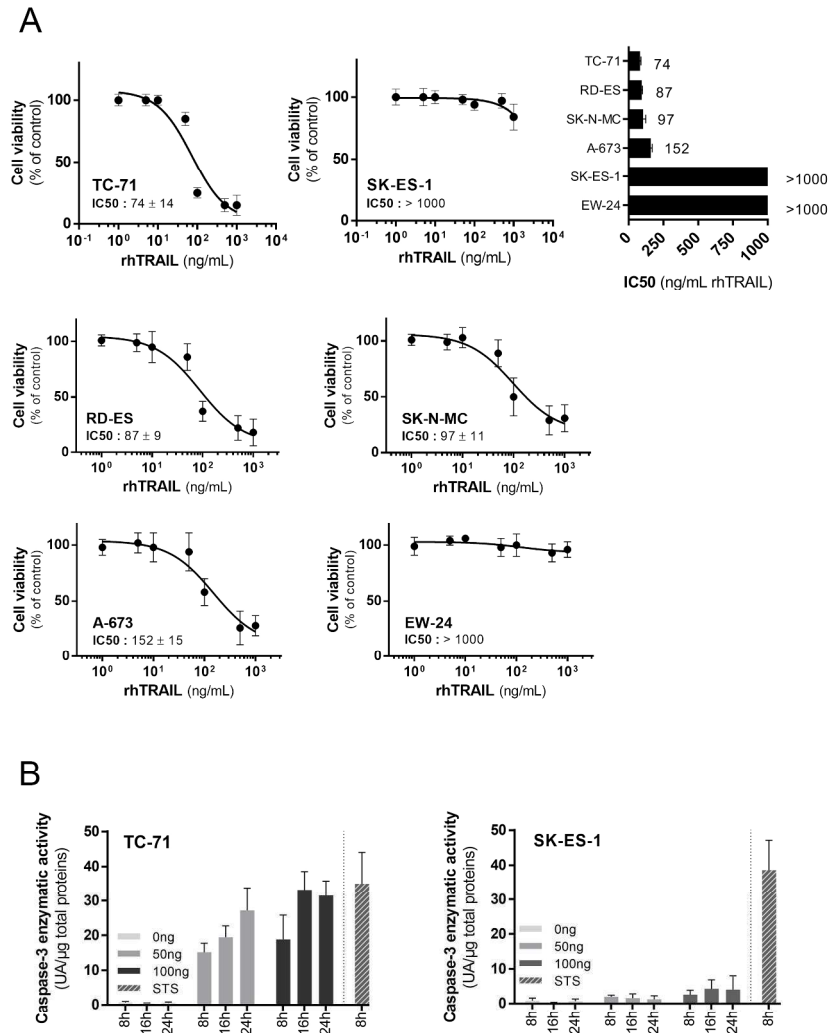


Figure 2. In vitro characterization of rhTRAIL effects on Ewing sarcoma (EWS) cells.
 A. rhTRAIL IC₅₀ was evaluated in EWS cell lines by WST-1 proliferation assay after 72h of culture.
 B. Apoptosis of TC-71 and SK-ES-1 cell lines determined after 8h or 16h of 50ng or 100ng rhTRAIL treatment, by quantification of caspase-3 enzymatic activity; TC-71 is a sensitive cell line model whereas SK-ES-1 is a resistant cell line model.

Figure 2
 209x297mm (300 x 300 DPI)

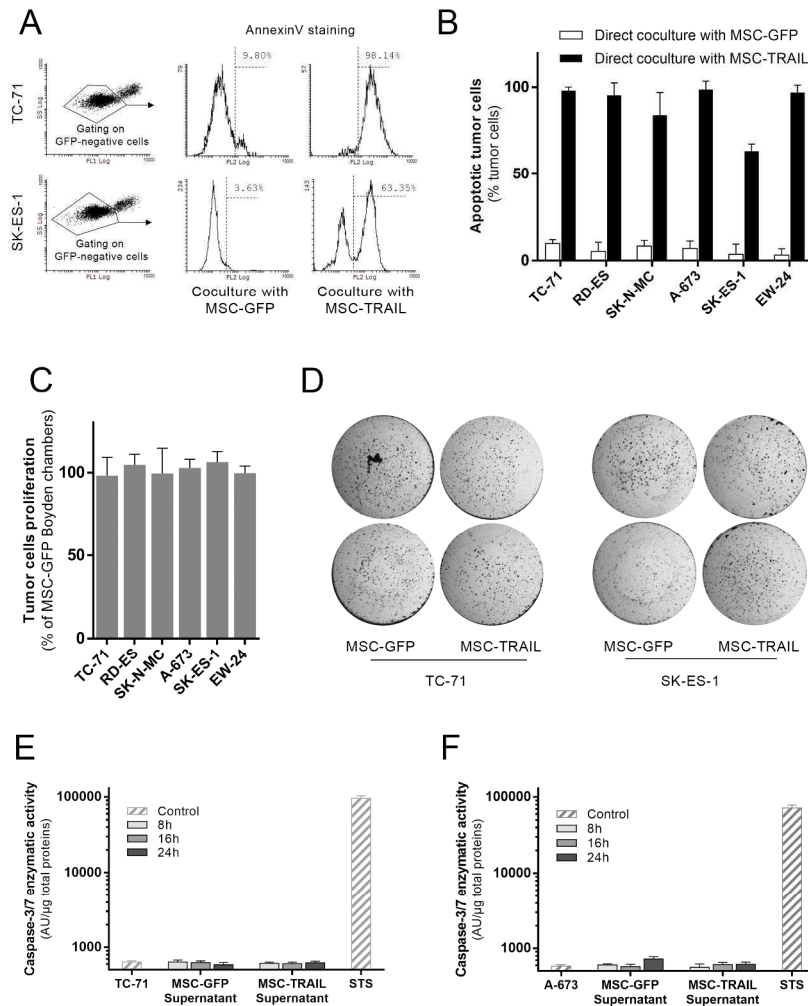


Figure 3. In vitro characterization of the effects of MSC-TRAIL on Ewing sarcoma cells.!! + A. Apoptosis of TC-71 or TC-32 cells co-cultured with MSC-GFP or MSC-TRAIL (tumor cell/MSC ratio of 3:1) was analyzed by AnnexinV cytometry assay gating of GFP-negative cells after 48h of co-culture.!! + B. Apoptosis of EWS cell lines co-cultured with MSC-GFP (light bars) or MSC-TRAIL (dark bars) was analyzed by AnnexinV cytometry assay after 48h of culture.!! + C. Tumor cell proliferation in Boyden chambers overhanging MSC-TRAIL for 48h was evaluated by crystal violet staining and reported as a percentage of Boyden chambers overhanging MSC-GFP.!! + D. TC-71 and TC-32 colonies on Boyden chambers overhanging MSC-TRAIL or MSC-GFP after 48h of culture are stained by crystal violet.!! + E. Caspase 3/7 activity in TC-71 cell lysate, relative to total protein, after 8h, 16h and 24h of treatment with MSC-GFP or -TRAIL supernatant.!! + F. Caspase 3/7 activity in A-673 cell lysate, relative to total protein, after 8h, 16h and 24h of treatment with MSC-GFP or -TRAIL supernatant.

Figure 3
209x297mm (300 x 300 DPI)

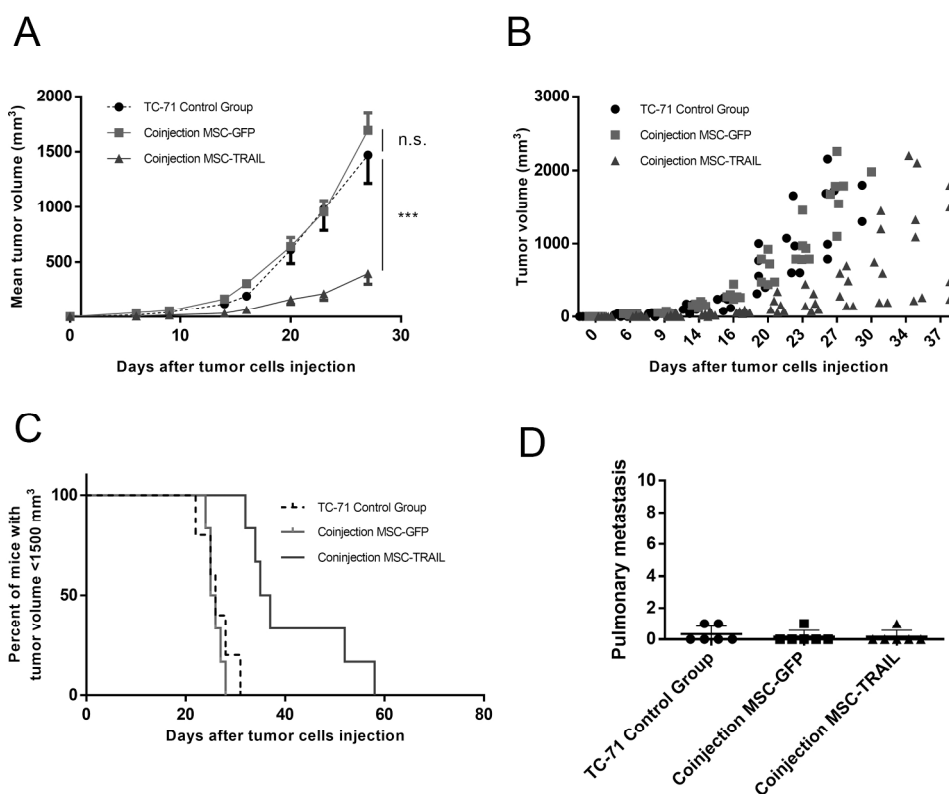


Figure 4. MSC-TRAIL co-injection prevents tumor development and increases mouse survival in the TC-71 Ewing sarcoma orthotopic xenograft model. Three groups of six mice were injected with 1 million TC-71 cells with or without 1 million MSC-GFP or -TRAIL as described in the "Materials and Methods" section.

A. Mean tumor volume per group

B. Tumor volumes per individual mouse

C. Mouse survival was defined as the percentage of mice with tumor volumes of less than 1500 mm³ in the three groups. (** p < 0.005; *** p < 0.001)

D. Number of macroscopic pulmonary metastases.

Figure 4

209x176mm (300 x 300 DPI)

Acc